# Precision deposition of a nanofibre by near-field electrospinning

**6 authors**, including:

Gaofeng Zheng
Xiamen University
**107** PUBLICATIONS   **566** CITATIONS

SEE PROFILE

Xiang Wang
Chinese Academy of Sciences
**98** PUBLICATIONS   **928** CITATIONS

SEE PROFILE

Dezhi Wu
Xiamen University
**70** PUBLICATIONS   **604** CITATIONS

SEE PROFILE

Daoheng Sun
Xiamen University
**193** PUBLICATIONS   **1,311** CITATIONS

SEE PROFILE

Some of the authors of this publication are also working on these related projects:

Near field electrospinning View project

# Precision deposition of a nanofibre by near-field electrospinning

**Gaofeng Zheng**[1,6]**, Wenwang Li**[1,2,6]**, Xiang Wang**[1]**, Dezhi Wu**[1,3]**, Daoheng Sun**[1,5] **and Liwei Lin**[1,4,5]

[1] Department of Mechanical and Electrical Engineering, Xiamen University, Xiamen 361005, People's Republic of China
[2] Department of Mechanical Engineering, Xiamen University of Technology, Xiamen 361005, People's Republic of China
[3] Department of Aeronautics, Xiamen University, Xiamen 361005, People's Republic of China
[4] Berkeley Sensor and Actuator Center, Department of Mechanical Engineering, University of California, Berkeley, CA 94720, USA

E-mail: sundh@xmu.edu.cn (D H Sun) and lwlin@me.berkeley.edu (L W Lin)

## Abstract

The deposition behaviour of an individual nanofibre on planar and patterned silicon substrates is studied using near-field electrospinning (NFES). A high-speed camera was utilized to investigate the formation and motion process of a liquid jet. Thanks to the shorter distance from the spinneret to the collector, bending instability and splitting of the charged jet in electrospinning were overcome. In NFES, a straight-line jet between the spinneret and the collector can be utilized to direct-write an orderly nanofibre. Perturbation stemming from residual charges on the collector caused the oscillation of the charged jet, and the deposition of the non-woven nanofibre on the planar substrate. With increasing collector speed, the impact of residual charges was weakened by the strong drag force from the collector and a straight-line nanofibre could be obtained. In addition, the nanofibre can be direct-written in a special pattern by controlling the motion track of the collector. Therefore, it can be concluded that a micro-strip pattern was a good guidance for nanofibre deposition, and the nanofibre deposition track followed well along the top surface of the micro-strip pattern. The position-controlled deposition of a single nanofibre provides a new aspect for applications of electrospinning.

(Some figures in this article are in colour only in the electronic version)

## 1. Introduction

Electrospinning is a cost-effective and versatile process to fabricate nanofibres from viscoelastic solutions at room temperature and atmospheric pressure, of which the diameter ranges from tens of nanometres to a few micrometres [1–3]. With numerous advantages such as smaller diameter, high surface-to-volume ratio and easy to process [4, 5], electrospinning has great potential applications in various fields, such as filtration membranes [6], composite reinforcement [7], optical devices [8] and bio-scaffolds [9].

In the conventional electrospinning process, a polymer solution pendant under the spinneret forms the Taylor cone shape due to the electrostatic field force. If the applied voltage reaches a critical value, the electrostatic force overcomes the surface tension and a charged jet of fluid emanates from the apex of the Taylor cone. After a short straight path directed towards the collector, the charged jet steps into the instability motion and splitting process. The instability process of electrospinning results in random nanofibre mats on the collector [10]. A well-controlled pattern could assist the nanofibre into different application fields, and several methods have been developed to control the deposition of a nanofibre, such as wheel-like reel [11], parallel array [12], electrostatic lens element [13] and assistant magnetic field [14]. However, these methods failed to provide the necessary location precision, which is of considerable demand in applications of microelectromechanical systems (MEMS) [15], organic

[5] Authors to whom any correspondence should be addressed.
[6] These authors contributed equally to this work.

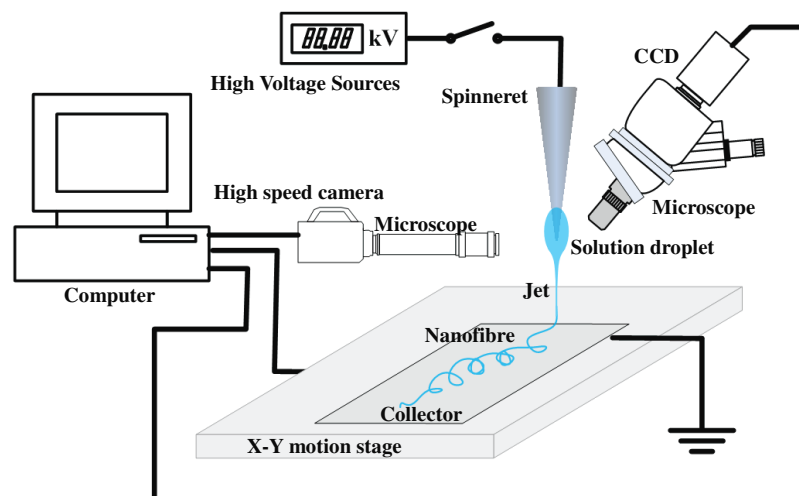J. Phys. D: Appl. Phys. **43** (2010) 415501

G Zheng *et al*

**Figure 1.** Schematic of experimental setup for NFES.

electronics [16], micro/nanosensors [17], power generators [18], etc.

Near-field electrospinning (NFES) [19] is a novel way to fabricate orderly nanofibres on flat substrates and realize patterned deposition of nanofibres. Hellmann *et al* discussed the impact of NFES processing parameters on the deposition morphology of nanofibres and non-woven nanofibres were deposited precisely along a predetermined pattern [20]. Chang *et al* developed continuous NFES to deposit solid nanofibres with orderly patterns over large areas, by which complex patterns could be assembled on a flat area [21]; they also direct-wrote a piezoelectric polymeric nanogenerator with high energy conversion efficiency by polyvinylidene fluoride (PVDF) based on NFES [18], which converted mechanical energy into electrical energy. Rinaldi *et al* used NFES to grow well-aligned parallel $TiO_2$ nanofibres on planar substrates [22], by which the sensing sensitivity and charge transferring efficiency of $TiO_2$ nanofibres were increased. Nanofibres as building blocks in the micro/nanosystem are one of the main development trends for electrospinning technology [23, 24], and precision deposition of nanofibres on pre-produced substrates is another great challenge to realize integrated nanofibres in micro/nanosystems.

In this paper, NFES was utilized to study the deposition behaviour of a single nanofibre, as well as the precise deposition of the nanofibre on patterns pre-produced on a silicon substrate.

## 2. Experiment

The experimental setup for NFES is represented in figure 1, which includes a solid probe spinneret, a high potential power supply, a collector, an $X-Y$ motion stage, two microscopes, a high-speed camera and a CCD camera. The diameter of the solid probe tip was $40 \mu$m. The anode of the high potential power supply (DW-P403-1AC, Tianjing Dongwen High Voltage Power Supply Plant, China) was connected to the probe, and the cathode was connected to the grounded silicon substrate. The applied voltage between the spinneret and the

collector can be adjusted from 0 to 40 kV. The collector was put on the $X-Y$ motion stage (TR10&TR07, Parker, USA), of which repetitive positioning accuracy, maximum acceleration and motion speed are $2 \mu$m, 5 g and $0-1$ m s$^{-1}$, respectively; the motion track of the stage can be controlled by a computer. Two microscopes were used in this experimental setup; one was used to observe the position of the spinneret above the collector, through which the CCD camera (Sony SSC-DC80, Japan) was used to record the images; the other one was fixed in front of the high-speed camera (GX-1, NAC Image Technology Inc, Japan) to observe the formation and motion process of the charged jet. A coaxial light source (Axen Light Source, L-150W, Taiwan, China) was used in the microscope systems. Polyethylene oxide (PEO, average molecular weight $= 300\,000$ g mol$^{-1}$, Dadi Fine Chemical Co., Ltd, China) solutions in 60/40 v/v water/ethanol were used as electrospinning materials.

The experiment was carried out under the optical microscope: the position of the spinneret above the collector was adjusted, which can be adjusted precisely with the help of a microscope; the tip of the solid probe spinneret was dipped into the polymer solution to draw out a discrete droplet, then a high potential was applied between the spinneret and the collector. The collector moved in the pre-programmed track under the control of a host computer. Under a high potential, the polymer jet was ejected out from the tip and a nanofibre was deposited on the collector. The diameter of the discrete droplet at the spinneret was about $50-60 \mu$m, and each droplet can be electrospun for $8-10$ s. The concentrations of the PEO solutions used in this work were 16% and 18%, of which the viscosities were about 26.5 Pa s and 80.5 Pa s, respectively. A viscoelastic solution, which has a high viscosity and good adhesion with the probe, would not drop out by the force of gravity.

The direct-written nanofibre was characterized by scanning electron microscopy (SEM) (LEO 1530 field-emission scanning electron microscope and XL30 field-emission environmental scanning electron microscope). Before the observation of SEM, the samples were sputter-coated with a gold layer of about 10 nm thickness.
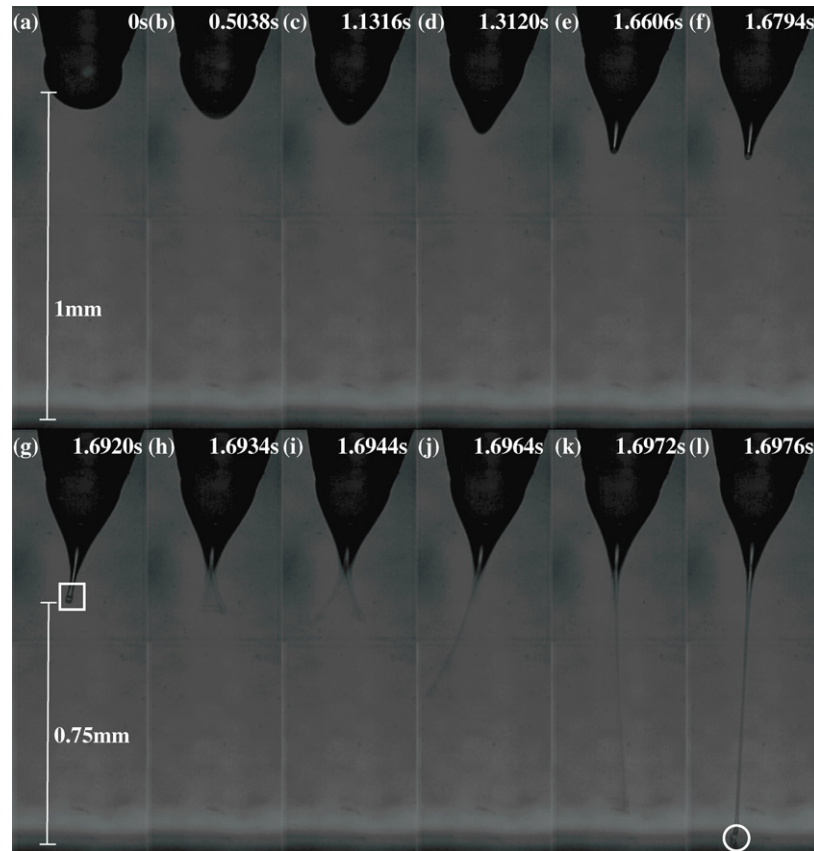
**Figure 2.** Formation and motion process of charged jet in NFES. Spinneret to collector distance, applied voltage and polymer solution concentration are 1 mm, 1.7 kV and 18%, respectively.

## 3. Results and discussion

### 3.1. Charged jet

The formation and motion process of the charged jet in NFES were recorded by the high-speed camera, as depicted in figure 2. The frame rate and exposure time of the high-speed camera were 5000 fps and 0.2 ms, respectively. Under sufficient applied voltage, the spherical liquid droplet on the tip of the spinneret was deformed into a Taylor cone, as shown in figures 2(*a*)–(*c*). Then, a straight jet ejected from the apex of the Taylor cone and moved towards the collector, as shown in figures 2(*f*)–(*l*).

Before the ejection of the liquid jet, charges accumulated on the surface of the solution droplet [25–27] under the high voltage potential between the spinneret and the collector. As the jet ejected from the apex of the Taylor cone, the excess charge accumulated on the solution droplet was carried away by the liquid jet. With the excess accumulated charge and larger electrical field force, the liquid jet dragged out more polymer solution and formed a small droplet in the front (the rectangle in figure 2(*g*)).

The charge repulsive force, which stemmed from charges carried by the adjacent part of the jet, imported lateral perturbation on the motion of the charged jet [26]. Due to the growth of perturbation from the charge repulsive force, the straight charged jet developed into a pendulum-like motion [28] after a short distance from the apex of the Taylor cone, as shown in figure 2(*h*). The front end of the jet oscillated

and stretched under the influence of the electrical field and the jet diameter decreased. It is observed that the swinging displacement of the charged jet increased from figure 2(*h*) to figure 2(*j*). When the charged jet extended further to the collector, the jet oscillating movement was weakened by the electric field pointed downwards to the collector. The displacement of oscillating movement decreased from figure 2(*j*) to figure 2(*k*). The deposition point of the charged jet is shown by a small circle in figure 2(*l*). It was 5.6 ms from figure 2(*h*) to figure 2(*l*), and the average motion speed of the charged jet was about 0.14 m s$^{-1}$.

After the ejection of the charged jet, a new balance between the electric field force and surface tension was built up and electrospinning went into the stable ejection process. The longitudinal stress caused by the electric field force would keep the charged liquid jet in the stable state [29–31], and the charged jet moved in a nearly straight line for a short distance from the apex of the spinneret. In NFES, the spinneret to collector distance shortened to 0.5–3 mm, and the nanofibre was collected before the bending and splitting happened. The straight charged jet between the spinneret and the collector in figure 2(*l*) can be utilized for direct-written nanofibres.

### 3.2. Nanofibre deposition on a planar substrate

The small droplet at the front end of the jet was deposited on the collector as shown in figure 2(*l*). After this initial stage,
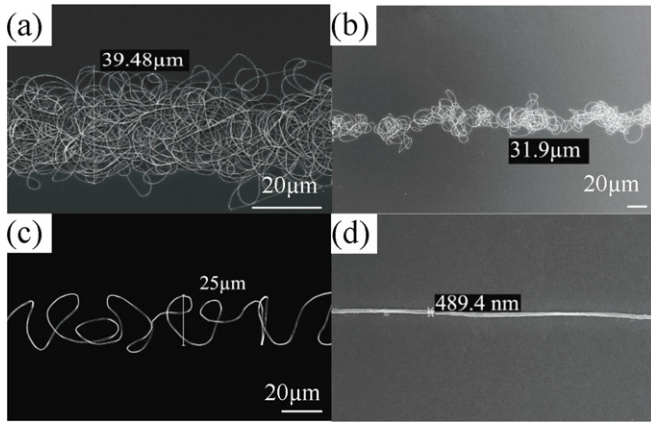
**Figure 3.** Nanofibre deposited on a planar silicon substrate by NFES. Collector speeds are (*a*) 0.03 m s$^{-1}$; (*b*) 0.08 m s$^{-1}$; (*c*) 0.20 m s$^{-1}$; (*d*) 0.36 m s$^{-1}$. Spinneret to collector distance, applied voltage and polymer solution concentration are 1 mm, 1.7 kV and 18%, respectively.



**Figure 4.** (*a*) Nanofibre deposited in 'U' shape; (*b*) close view of nanofibre deposited at the corner of the 'U'-shaped structure. Spinneret to collector distance, applied voltage, polymer solution concentration and collector speed are 1 mm, 1.5 kV, 18% and 0.10 m s$^{-1}$, respectively.



**Figure 5.** Nanofibre deposited on a patterned silicon substrate at different collector speeds. Collector speed is 0.25 m s$^{-1}$ for nanofibres $\alpha$ and $\gamma$, 0.35 m s$^{-1}$ for nanofibres $\beta$ and $\delta$. Spinneret to collector distance, applied voltage and polymer solution concentration are 1 mm, 1.7 kV and 18%, respectively. Open arrows show the collector motion direction.

a stable fine jet was formed and the diameter of the stable jet was smaller than that of the initial droplet. The stable jet with smaller diameter resulted in a solid nanofibre deposited on the planar silicon substrate.

Collector speed is one of the important process parameters that affects the nanofibre deposition in NFES [32]. Various patterns can be constructed by adjusting the collector speed. When the charged nanofibre was deposited on the silicon substrate, residual charges on the substrate could affect the deposition behaviour. Specifically, when the collector speed was lower than the ejection speed of the jet stream (the average speed of the charged jet is 0.14 m s$^{-1}$ in figure 2), the jet/nanofibre was easily affected by the repulsive force from the residual charges and resulted in oscillation motion [28]. Nanofibre deposition was in a non-woven pattern on the planar silicon substrate, as shown in figures 3(*a*) and (*b*). Collector speeds in figures 3(*a*) and (*b*) were 0.03 m s$^{-1}$ and 0.08 m s$^{-1}$, respectively. As the collector speed increased, the drag force from the collector could reduce the width and density of the nanofibre. When the collector speed was 0.20 m s$^{-1}$, a nanofibre with a helical shape was deposited in a narrower zone as shown in figure 3(*c*). When the collector speed was 0.36 m s$^{-1}$, the oscillation motion of the charged jet/nanofibre disappeared and a straight-line nanofibre without the helical structure was obtained, as shown in figure 3(*d*).

In NFES, nanofibres deposited in different patterns can be obtained by adjusting the moving speed of the collector [19, 21]. Computer controlled movement of the collector resulted in a deposited single nanofibre in 'U' shape as shown in figure 4(*a*). The collector was stopped at the corner for 0.2 s to change the moving direction, and excessive nanofibres were deposited at the corner, as shown in figure 4(*b*). The balance between the charge repulsive force and the elastic force inside the nanofibre, which was built up during the stable electrospinning process [33], resulted in spiral nanofibres in the straight track.
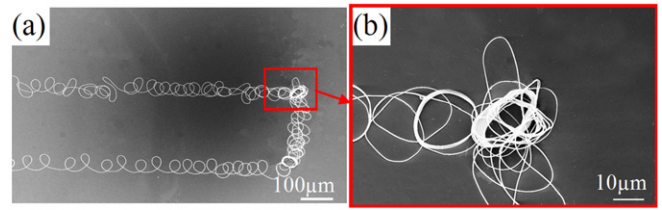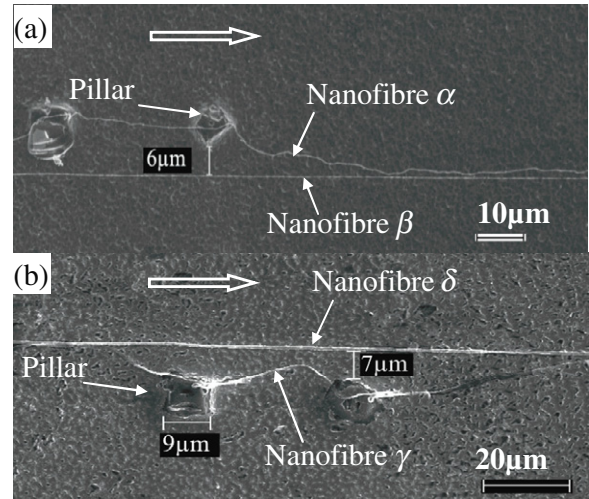
### 3.3. Nanofibre deposition on a patterned substrate

A patterned silicon substrate was used as the collector to study the deposition process by NFES. When the collector moved twice at different speeds, two nanofibres were direct-written on the patterned substrate, as shown in figure 5. When the collector speed was 0.25 m s$^{-1}$, the nanofibre moved away from its original track towards the micro-pattern (nanofibres $\alpha$ and $\gamma$ in figure 5), and the offset values of nanofibres $\alpha$ and $\gamma$ were 6 $\mu$m and 7 $\mu$m, respectively. When the collector speed was 0.35 m s$^{-1}$, the silicon micro-pattern seemed to have little impact on the deposition of nanofibres probably due to the stronger drag force from the collector. The deposition track of the nanofibre (nanofibres $\beta$ and $\delta$ in figure 5) maintained a straight line.

The deposition precision of the nanofibre is better than 1 $\mu$m and the nanofibre can be direct-written accurately across the micro-pillars, as shown in figure 6. At a collector speed of 0.35 m s$^{-1}$, nanofibres with a straight-line pattern were deposited along the micro-pillar array (figures 6(*a*) and (*b*)). The diameters of the micro-pillar were 9.08 $\mu$m and 1.6 $\mu$m in figures 6(*a*) and (*b*), respectively. As the collector speed and the drag force of the collector decreased, nanofibres aggregated on the top surface of the micro-pattern under the electrical field
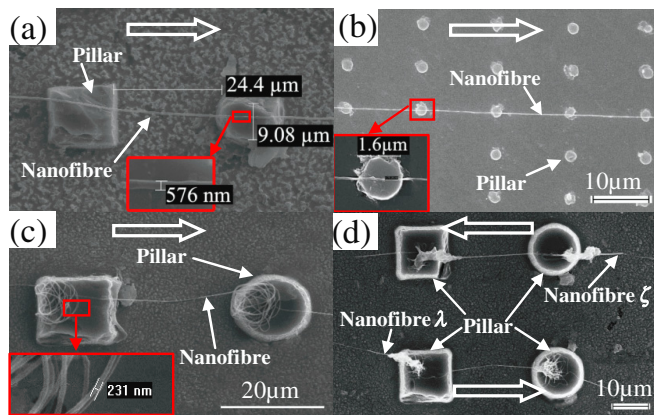
**Figure 6.** Nanofibre deposited on the patterned substrate with micro-pillar. Collector speeds are (*a*) and (*b*) 0.35 m s$^{-1}$; (*c*) and (*d*) 0.2 m s$^{-1}$. Polymer solution concentrations are (*a*)–(*c*) 18%; (*d*) 16%. Spinneret to collector distance and applied voltage are 1 mm and 1.7 kV, respectively. Open arrows show the collector motion direction.
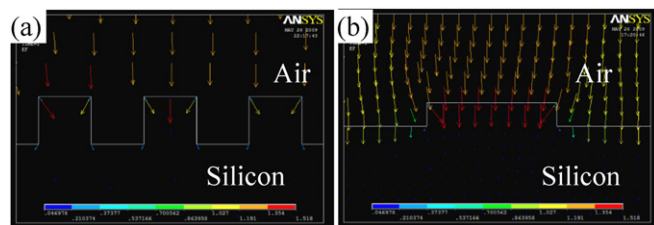


**Figure 7.** Simulation of electric field distribution above the patterned silicon substrate. (*a*) Electric field above micro-pattern array; (*b*) electric field above single micro-pattern.

force, as shown in figures 6(*c*) and (*d*). The polymer solution concentration was another important factor that defined the deposition morphology of nanofibres. If the solvent in the jet did not evaporate adequately, the aggregated nanofibre on the top surface of the micro-pattern coagulated into a polymer bundle as illustrated in figure 6(*d*) where the polymer solution concentration was 16%. However, it is observed that the solid nanofibres aggregated on the top surface of the micro-pattern did not coagulate in figure 6(*c*), where the polymer solution concentration was 18%.

In order to further investigate the effect of micro-pattern on the nanofibre deposition process, the electric field distribution above the patterned silicon substrate was simulated, as shown in figure 7. The simulation results show that the electrical field strength above the micro-pattern is stronger than other areas. In this work, the anode of the high potential power supply was connected to the spinneret, and the liquid jet carried away positive charges from the spinneret. The electric field above the patterned silicon substrate could move away the charged jet from its original deposition track towards the surface of the micro-pattern due to the stronger electrical field. Furthermore, the nanofibre could aggregate on the top surface of the micro-pattern under the electric field force, as shown in figures 6(*c*) and (*d*) if the collector moving speed was low.

Straight-line patterns can be used to guide the deposition of nanofibres because of the stronger electrical field, as shown in figure 8. Similarly to direct-writing on a planar substrate,
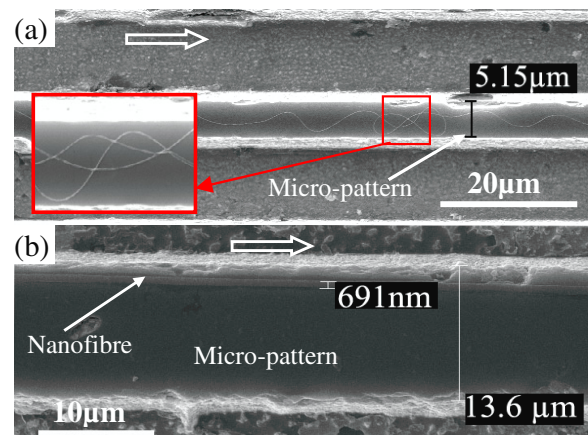


**Figure 8.** Nanofibre deposited along the top surface of straight-line-shaped micro-patterns. Collector speeds are (*a*) 0.2 m s$^{-1}$; (*b*) 0.35 m s$^{-1}$. Spinneret to collector distance, applied voltage and polymer solution concentration are 1 mm, 1.7 kV and 18%, respectively. Open arrows show the collector motion direction.

nanofibres in spiral shape (0.2 m s$^{-1}$ in figure 8(*a*)) and straight line (0.35 m s$^{-1}$ in figure 8(*b*)) can be fabricated on the top surface of a micro-strip pattern with different collector speeds. It is observed that the nanofibre was restricted to be deposited on the top surface of the micro-pattern only. The width of the nanofibre deposition zone was 5.15 $\mu$m in figure 8(*a*), which was narrower than the deposition result on a planar substrate (25 $\mu$m in figure 3(*c*)) at the same collector speed.

Micro-patterns with an arc shape were also tested. In this study, the collector moved in a straight line, but nanofibre deposition was deviated from the original straight line and deposition occurred along the top surface of the arc, as shown in figure 9. The width of the micro-strip pattern was 1 $\mu$m. Therefore, a patterned substrate could be a good way to increase the deposition precision of direct-written nanofibres for integrating nanofibres accurately with other micro/nanostructures.

## 4. Conclusions

NFES was used to study the position control of nanofibres. In the initial jet-stream formation process, a charged jet oscillated outside the apex of a liquid Taylor cone. As the jet stream approached the collector, oscillating movement of the jet stream was reduced and a straight jet stream was formed when the tip of the jet stream was in contact with the collector substrate. With the help of a microscope, the position of the probe above the substrate can be adjusted accurately to control the deposition positions of nanofibres.

The residual charges accumulated on the collector caused nanofibres to move away from their original deposition points. If the collector moved fast enough, a mechanical drag force was generated on the suspended nanofibre from the collector. Furthermore, the width and density of the deposited nanofibres decreased when the speed of the collector increased. When the collector speed matched the jet motion speed, line-shaped nanofibres could be constructed. Therefore, the deposition
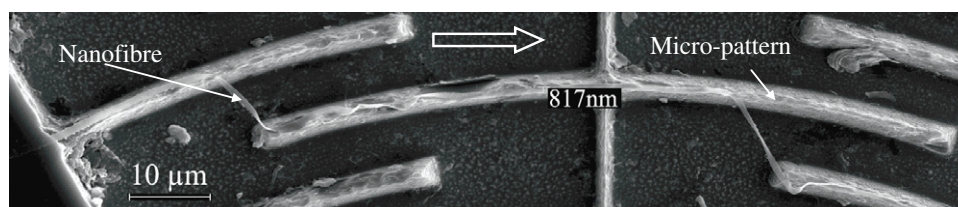
**Figure 9.** Nanofibre deposited along the arc micro-pattern. Spinneret to collector distance, applied voltage, polymer solution concentration and collector speed are 1 mm, 1.7 kV, 18% and 0.30 m s$^{-1}$, respectively. Open arrow shows the collector motion direction.

patterns of nanofibres can be controlled well by adjusting the motion speed of the collector.

Patterned silicon structures can increase the deposition precision of nanofibres. Experimentally, the nanofibre by NFES had a good position precision of 1 $\mu$m on a patterned silicon collector with micro-pillar array or micro-strip patterns. These extruded microstructures have stronger electric fields to attract the nanofibre. At lower collector speeds, the nanofibre aggregated on the top surface of the micro-patterns under the electric force. Since nanofibres by NFES can be deposited on a patterned substrate with very good precision, it provides a unique way for the precision deposition and integration of nanofibres with micro/nanosystems, in the fields of MEMS, micro-sensors, power devices, etc.

## Acknowledgments

## References

[1] Nisbet D R, Forsythe J S, Shen W, Finkelstein D I and Horne M K 2009 *J. Biomater. Appl.* **24** 7

[2] Bhattacharjee P K, Schneider T M, Brenner M P, McKinley G H and Rutledge G C 2010 *J. Appl. Phys.* **107** 044306

[3] Yang C, Jia Z, Guan Z and Wang L 2009 *J. Power Sources* **189** 716

[4] Lee H, Choi S H, Jo S M, Kim D Y, Kwak S, Cha M W, Kim I D and Jang S Y 2009 *J. Phys. D: Appl. Phys.* **42** 125409

[5] Feng C, Khulbe K C and Matsuura T 2010 *J. Appl. Polym. Sci.* **115** 756

[6] Heikkila P, Taipale A, Lehtimaki M and Harlin A 2008 *Polym. Eng. Sci.* **48** 1168

[7] Liu L Q, Eder M, Burgert I, Tasis D, Prato M and Wagner H D 2007 *Appl. Phys. Lett.* **90** 083108

[8] Yang G C, Gong J, Pan Y, Cui X J, Shao C L, Guo Y H, Wen S B and Qu L Y 2004 *J. Phys. D: Appl. Phys.* **37** 1987

[9] Meechaisue C, Wutticharoenmongkol P, Waraput R, Huangjing T, Ketbumrung N, Pavasant P and Supaphol P 2007 *Biomed. Mater.* **2** 181

[10] Kong C S, Yoo W S, Jo N G and Kim H S 2010 *J. Macromol. Sci. B: Phys.* **49** 122

[11] Katta P, Alessandro M, Ramsier R D and Chase G G 2004 *Nano Lett.* **4** 2215

[12] Li D, Wang Y and Xia Y 2004 *Adv. Mater.* **16** 361

[13] Deitzel J M, Kleinmeyer J D, Hirvonen J K and Beck Tan N C 2001 *Polymer* **42** 8163

[14] Wong S-C, Baji A and Leng S 2008 *Polymer* **49** 4713

[15] Czaplewski D, Kameoka J and Craighead H G 2003 *J. Vac. Sci. Technol.* B **21** 2994

[16] Lee S W, Lee H J, Choi J H, Koh W G, Myoung J M, Hur J H, Park J J, Cho J H and Jeong U 2010 *Nano Lett.* **10** 347

[17] Wang X Y, Drew C, Lee S H, Senecal K J, Kumar J and Sarnuelson L A 2002 *Nano Lett.* **2** 1273

[18] Chang C, Tran V H, Wang J, Fuh Y-K and Lin L 2010 *Nano Lett.* **10** 726

[19] Sun D H, Chang C, Li S and Lin L W 2006 *Nano Lett.* **6** 839

[20] Hellmann C, Belardi J, Dersch R, Greiner A, Wendorff J H and Bahnmueller S 2009 *Polymer* **50** 1197

[21] Chang C, Limkrailassiri K and Lin L W 2008 *Appl. Phys. Lett.* **93** 123111

[22] Rinaldi M, Ruggieri F, Lozzi L and Santucci S 2009 *J. Vac. Sci. Technol.* B **27** 1829

[23] Ishii Y, Sakai H and Murata H 2008 *Mater. Lett.* **62** 3370

[24] Kameoka J, Orth R, Yang Y N, Czaplewski D, Mathers R, Coates G W and Craighead H G 2003 *Nanotechnology* **14** 1124

[25] Reneker D H and Yarin A L 2008 *Polymer* **49** 2387

[26] Reneker D H, Yarin A L, Zussman E and Xu H 2007 *Adv. Appl. Mech.* **41** 43

[27] Yarin A L, Koombhongse S and Reneker D H 2001 *J. Appl. Phys.* **90** 4836

[28] Han T, Reneker D H and Yarin A L 2008 *Polymer* **49** 2160

[29] Hohman M M, Shin M, Rutledge G and Brenner M P 2001 *Phys. Fluids* **13** 2201

[30] Hohman M M, Shin M, Rutledge G and Brenner M P 2001 *Phys. Fluids* **13** 2221

[31] Jaworek A 2008 *J. Microencapsul.* **25** 443

[32] Zheng G F, Wang L Y, Wang H L, Sun D H, Li W W and Lin L W 2009 *Adv. Mater. Rev.* **60–61** 439

[33] Kim H-Y, Lee M, Park K J, Kim S and Mahadevan L 2010 *Nano Lett.* **10** 2138